



HAL
open science

Adapting the available water capacity indicator to forest soils: An example from the Haut-Languedoc (France)

Baptiste Algayer, Philippe Lagacherie, Jean Lemaire

► To cite this version:

Baptiste Algayer, Philippe Lagacherie, Jean Lemaire. Adapting the available water capacity indicator to forest soils: An example from the Haut-Languedoc (France). *Geoderma*, 2020, 357, 10.1016/j.geoderma.2019.113962 . hal-02623221

HAL Id: hal-02623221

<https://hal.inrae.fr/hal-02623221>

Submitted on 9 Sep 2021

HAL is a multi-disciplinary open access archive for the deposit and dissemination of scientific research documents, whether they are published or not. The documents may come from teaching and research institutions in France or abroad, or from public or private research centers.

L'archive ouverte pluridisciplinaire **HAL**, est destinée au dépôt et à la diffusion de documents scientifiques de niveau recherche, publiés ou non, émanant des établissements d'enseignement et de recherche français ou étrangers, des laboratoires publics ou privés.



Distributed under a Creative Commons Attribution - NonCommercial - NoDerivatives 4.0 International License

1 **Confronting the available water content indicator to forest soils: the example**
2 **from the Haut-Languedoc (France).**

3 Algayer Baptiste ¹, Lagacherie Philippe ², Lemaire Jean ³

4 ¹Parc naturel régional du Haut-Languedoc, 1 place du Foirail, BP9, 34220 Saint-Pons de
5 Thomières.

6 ²LISAH, Université de Montpellier, IRD, INRA, Montpellier SupAgro, place Viala, 34060
7 Montpellier.

8 ³Institut pour le Développement Forestier, 175 cours Lafayette, 69006 Lyon.

9

10 **Highlight:**

- 11 - The soil available water content (SAWC) calculation needs specific adjustments when
12 applied to forest soils.
- 13 - The considered soil volume is the main driver of SAWC
- 14 - The soil coarse fraction contains available water for plant, and this amount of water
15 must be considered in soil available water content assessment.
- 16 - Specific pedotransfert functions are needed for the fine earth water retention
17 assessment of forest soils.

18

19 **Abstract:**

20 Soil available water content (SAWC) is becoming a crucial issue for forest management in the
21 context of climate changes. Nevertheless, SAWC indicator which was created for agricultural
22 soils needs specific adaptations when it is estimated for forest soils. This study aimed to find
23 the best way to apply the SAWC indicator with regard to its significance for explaining
24 variations of tree fertility across a given region. An extensive study over a spatial sampling of

25 100 Douglas-fir stand plots was conducted in the Haut Languedoc Regional Nature Parc
26 (Southern France). It involved stand fertility assessments, morphological observations of deep
27 soil pits including the saprolite, quantitative estimations of coarse fragments, texture and
28 organic matter laboratory analysis and water retention and density measurements on a
29 limited sample of horizons (35). Different SAWC were computed from the collected data. They
30 differed in the methods i) for estimating the fine earth water retention – national vs local
31 pedotransfer function -, ii) for dealing with the coarse fragments – assumed to contribute or
32 not to the water retention of soils- and iii) for estimating the soil volumes – variable
33 thicknesses and considerations of rooting. The results showed that the SAWC that explained
34 the best the variations of tree fertilities over the study area (21% of the variance) was obtained
35 by fine earth water retention estimated from a local pedotransfert function, by considering
36 the water retention of the coarse fraction and by exploring the largest volumes (thicknesses
37 of 200 cm, 300 cm and equal to the depth to bedrock) without explicit consideration of the
38 rooting observations. The ranking of SAWC component impact on SAWC values was i) soil
39 volume, ii) coarse fraction water retention and iii) fine earth retention. Those results revealed
40 that improvements in estimating coarse fraction water retention and soil volumes, and, to a
41 lesser extent, in estimating fine-earth water retention by forest soil adapted pedotransfer
42 function, would greatly benefit to the application of the SAWC indicator to forest soils.

43 **Keywords:** soil available water capacity, forest soils, Douglas-fir, rock fragment water
44 retention, pédotransfert function.

45 1. Introduction

46 Soil available water capacity (SAWC) is a well-known concept that have been used for a long
47 time for expressing the capacity of soils to store water for plants (Veihmayer and Hendrickson,
48 1927). It has been demonstrated that SAWC is one of the most important soil factors for plant

49 growth, influencing photosynthesis rate, carbon allocation, and nutrient cycling (Lebourgeois
50 et al., 2005; Breda et al., 2006). It is therefore a first order parameter that is used in land
51 evaluations and recently in soil ecosystem service assessment (Dominati et al. 2014). For now,
52 in the literature, SAWC is expressed as follows (equation 1) (Cousin et al., 2003):

$$SAWC = \sum_{Hi} Thickness_{(Hi)} \times [(W_{(FC)} - W_{(WP)}) \times D]_{(Hi)} \times \frac{100 - CF}{CF}_{(Hi)} \quad (1)$$

53 Where H_i is the horizon i of the soil profile, $Thickness_{(H_i)}$ is the horizon thickness in
54 centimeters, $W_{(FC)}$ is the gravimetric water content at the field capacity for fine earth of the
55 horizon, $W_{(WP)}$ is the gravimetric water content at the wilting point for fine earth of the
56 horizon, D is the bulk density of the fine earth of the horizon, CF is volume of the coarse
57 fraction of the horizon in percentage. This equation can be divided in three components: i)
58 the fine earth water retention properties that is usually estimated by pedotransfert functions
59 (PTF) (Wösten et al., 2001; Bruand et al., 2003; Almajou et al., 2008) ii) the coarse fraction
60 volume, that is usually excluded from the equation considering that coarse fragments do not
61 contain available water and iii) the thickness of the material that weights the AWC of each
62 horizon through the soil profile.

63 SAWC concept has been created for crop field soils, but is also largely applied to forest soils
64 (Curt et al., 2001; Chen et al., 2002; Seynave et al., 2005; Piedallu et al., 2011). SAWC is
65 commonly used in combination with climatic and topographic data in order to predict site
66 fertility of a forest stand (Chen et al., 2002; Seynave et al., 2005). It is also used for soil water
67 balance calculation (Granier et al., 1999) in order to study the forest-stand response to
68 drought that is becoming a crucial issue in context of climate changes (Breda et al., 2006;
69 Sergent et al., 2012; Littke et al., 2018).

70 However, applying SAWC indicator to forest soils carries some difficulties related with the
71 specificities of forest soil and forest context. Firstly, trees are powerful plants whose roots
72 may colonize a greater soil thickness than cultivated plant. Many studies showed that
73 colonization by roots could go far beyond the soil, reaching the saprolite zone in which this
74 colonization can be very irregular (Curt et al., 1998; Graham et al., 2010; Brantley et al., 2017).
75 This makes not straightforward to define in equation 1 an appropriate value of thickness that
76 account for this heterogeneity. Second, by reaching the saprolite zone, forest soils often show
77 high coarse fraction volumes. It has been demonstrated that coarse fragment can store water
78 which could be available for plant (Flint and Childs, 1984; Tetegan et al. 2011; Parajuli et al.,
79 2017). When the proportion of coarse fragment becomes important, this could play a major
80 role in SAWC. Hence, equation 1 should be modified for taking into account the AWC of the
81 coarse fraction ($AWC_{(CF)}$). Lastly, the determination of the fine earth AWC ($AWC_{(FE)}$) has been
82 by far much more investigated than the two previously evoked components. To cope with
83 metrologic difficulties in measuring gravimetric water content at field capacity ($W_{(FC)}$) and at
84 wilting point ($W_{(WP)}$) there is a wide use of pedotransfer functions (PTF) (Jamagne et al., 1977;
85 Wösten et al., 2001; Almajou et al., 2008). However, most of these PTF have been developed
86 from agricultural soil measurements and to our knowledge, no specific PTF for forest soils
87 exists (Vincke and Delvaux, 2005; Piedallu et al., 2011). Piedallu et al (2018) promoted the use
88 of Almajou 2008' PTF which is derived from agricultural soils. The applicability of PTF to forest
89 soil remains unknown.

90 In this paper, we apply the concept of SAWC for characterizing the potential of growth of
91 Douglas-fir in the Haut Languedoc Regional Nature Parc (Southern France). Different
92 modalities for calculating the SAWC components are applied from a dataset of 100 deep soil

93 pits. The resulting SAWCs are evaluated with regard to their correlation with an indicator of
94 tree growth.

95 2. The study area and data

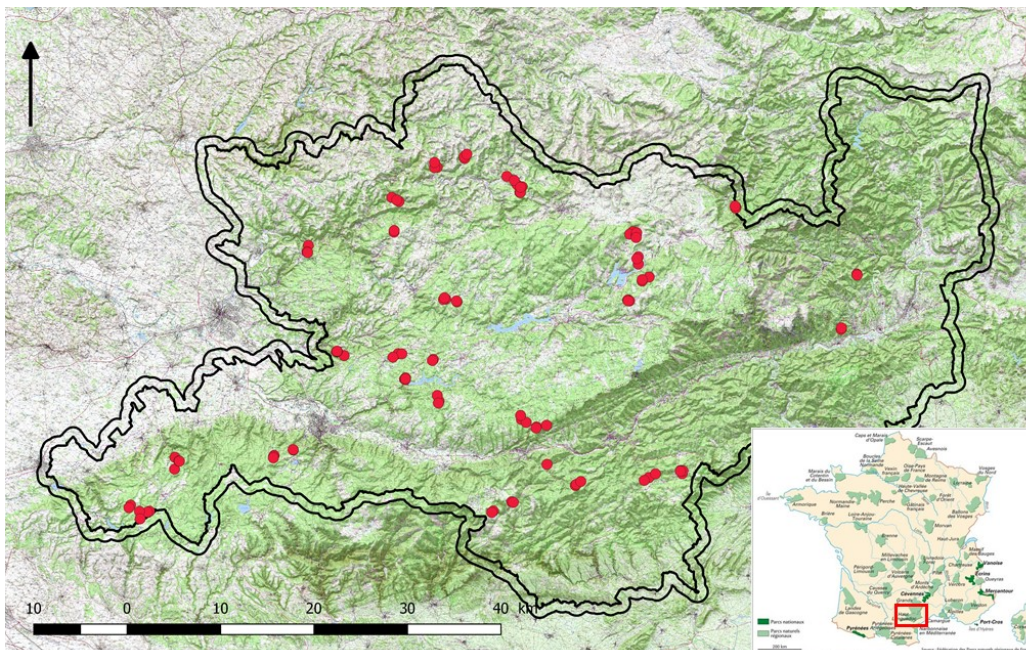
96 2.1. General description

97 The Haut Languedoc Regional Nature Park is a 314 000 hectares area located in the south of
98 France. This area is covered at 66% by forest, making wood production a crucial issue for the
99 region. The studied area lays through the confluence zone of three contrasted climates. At the
100 east, Mediterranean climate present an annual rainfall of 650mm, concentrated during
101 autumn and spring seasons, and is characterized by a high summer water deficit (-300mm). In
102 the west, oceanic climate is more humid (1650mm annual rainfall) with a more uniform
103 rainfall regime and a lower summer water deficit (-100mm). Finally, in the north, a semi-
104 mountain climate shows wetter and colder average conditions. Geology and topography are
105 also very heterogeneous. The south-west of the study area, called black mountain, is
106 composed on granitic and gneissic mountains reaching 1200 meters high. The center of the
107 area is composed on granitic and gneissic plateau ranging between 800 and 1100 meters high,
108 surrounded by schist and calcschist hills in the north west and schist and calcareous materials
109 in the south east. Such peripheric regions show lower altitude but very rugged terrain with
110 deep valleys and narrows crests. Such variability implies very heterogeneous forest soil type
111 distribution and thus, a large range of SAWC.

112 2.2. Plot sampling

113 A 100 plots sampling design was set up in order to exhaustively represent forest soils of the
114 studied area. The sampling design was performed on Douglas-Fir (*Pseudotsuga menziesii*)
115 plantations because this species is of high economic interest and is therefore widely
116 represented across the different climates and parent materials of the study area, which

117 ensures to get a large range of soil conditions. Sampling strategy was based on the
118 combination of climatic, geologic, and topographic classifications. Three sub-zones were
119 distinguished: the central mountain zone (mountain climate), the western zone (oceanic
120 climate) and the eastern zone (Mediterranean climate). Topography classification included
121 four topographic positions: plateau, top slope, mid slope and lower slope combined with three
122 exposition modalities (north, south and other). In the central zone, classification was based
123 on topographic conditions combined with an altitude threshold (800 meters). For the western
124 and eastern zones, topographic classification was combined with geologic classification: schist
125 and granites rocks in the western zone, schist and calcareous rocks in the eastern zone.
126 Sampling strategy also took into account practical conditions such as accessibility for a 25 tons
127 shovel, optimization of the shovel transport, and forest owner agreement.



128
129 *Figure 1: spatial distribution of the sampling plots in the studied area*

130 2.3. Soil observations

131 For each plot, a soil pit was dug using a 25 tons shovel. The soil pit was positioned at a two
132 meters distance from the tree localised at the centre of the trees spiral composing the plot.

133 Soil material was excavated until the inscrutable bedrock was reached. When bedrock was
134 too deep underground, the soil pit limit was 4.5 meters depth, corresponding on the maximum
135 accessible depth for the shovel mechanical arm. Soil profiles were visually described following
136 the French protocol of soil description (Infosol, 2018), including the measurement of the soil
137 horizons thickness. Sometimes the soil horizons presented a complex geometry i.e. non-
138 horizontal horizon limits, discontinuous, or enclosed horizons, into the saprolite zone. Non-
139 horizontal horizon limits were registered using the DONSOL protocol. Discontinuous and
140 enclosed horizons were considered as component of a complex horizons, which required to
141 modify the description protocol. Furthermore, graphical representations of each profiles were
142 performed to memorize the observed horizon complexity.

143 A particular attention was paid for characterizing coarse fraction, both quantitatively and
144 qualitatively. The classical estimation of the amount of coarse fragment from a visual
145 interpretation of the profile was replaced by a more precise technique that estimated
146 separately the gravel fraction (between 2mm and 2cm diameter) and the pebbles fraction
147 (more than 2 cm). The latter was determined in the field by a 2 cm sieving and weighing. The
148 determined fine earth and pebble densities were used to convert mass fraction into
149 volumetric fractions. The gravel fraction was determined in the laboratory from the 2cm-
150 sieved samples obtained from the previously evoked operation. The total coarse fraction was
151 obtained by adding the two previously determined fractions.

152 A total of 80 rock fragments were sampled for density and water retention measurement. The
153 sampling considered eight rock fragment types that corresponded to the mainly represented
154 lithologic classes of the studied area: mica-schist, black schist, shale, pelitic sandstone, banded
155 sandstone, dolomite, limestone, granite and gneiss. Ten samples of each lithologic class were
156 collected. The rock samples consisted of flat-shaped pebbles with a size varying between 3cm

157 and 6cm for the longer diameter. The samples were gently brushed prior measurement, in
158 order to remove their fine earth coatings.

159 Considering the fine earth, 200 grams samples were collected from each soil horizon in order
160 to measure five class particle size distribution and organic matter content. In addition,
161 undisturbed clods were sampled from 35 horizons (A and S horizons), for water retention
162 measurements. The sampled clods were chosen in order to exhaustively represent the soil
163 types of the studied area. The undisturbed clods were gently fragmented by hand in order to
164 form 5 cm diameter clods. The samples were kept in plastic boxes and stored at 4°C until
165 analyses.

166 2.4. Water retention and dry bulk density measurements

167 Rock fragments and clods gravimetric water content was determined at field capacity (-330
168 hPa) ($W_{(FC)}$) and at wilting point (-15000 hPa) ($W_{(WP)}$) following a classical protocol (ref).
169 Measurements were performed on a pressure membrane. After saturation by capillarity,
170 samples were placed on a paste of saturated kaolinite to obtain a sufficient hydraulic
171 continuity with the pressure membrane. After one week of equilibrium in pressure cells, the
172 gravimetric water content was measured.

173 Dry bulk density was estimated using the paraffin method (ref). Samples were dipped into
174 hot paraffin. By cooling, a thin paraffin coating was formed and blocked the sample pores.
175 Paraffin coated-samples were dipped into a water container, and the coated sample volume
176 was estimated by the water displacement. Finally, the paraffin coating was carefully removed
177 from the sample using a cutter. Paraffin residues were weighed and the volume of the coating
178 was calculated. The rock fragment bulk density was calculated by the difference between the
179 coated sample volume and the paraffin volume. The measurement of bulk density, gravimetric

180 water content at field capacity and wilting point were repeated and averaged on 10 different
181 samples for each fine earth horizon, and each rock fragment lithologic class.

182 Following the measurements, both fine earth and coarse fragment water retention properties
183 were calculated and summed up into an AWC coefficient (AWC_{coef}) calculated using the
184 following equation 3.

$$AWC_{coef} = (W_{(FC)} - W_{(WP)}) * D * 0.1 \quad (3)$$

185 Where $W_{(FC)}$ is the gravimetric water content at field capacity in mm, $W_{(WP)}$ is the gravimetric
186 water content at the wilting point in mm and D is the bulk density.

187 Coarse fraction AWC coefficient ($AWC_{coef(CF)}$) was calculated for the eight considered
188 lithologic classes. Fine earth AWC coefficient was calculated for the 35 sampled horizons
189 ($AWC_{coef(FE)}$).

190 2.5. Root measurements

191 For each soil profile, the depth of the deepest visible root was measured. At the horizon scale,
192 root density was estimated by counting. For each horizon, three 10*10 cm squares areas were
193 considered. The first square was localized on the highest root density zone of the horizon, the
194 second square on the lowest density zone and the third was localized on the medium root
195 density zone. For each square, visible roots with a diameter less than 2 cm, were counted and
196 classified by health status (healthy, dead).

197 2.6. Site fertility Index H50

198 A forest stand plot consisted of a 20 dominant trees spiral. Each diameter at breast height
199 (1.30 m) was measured. The dominant height of the three largest trees was measured using
200 a Vertex laser dendrometer. The age was measured using a Pressler increment borer. Site
201 fertility index was calculated for each stand at the reference age of 50 years ($H_{(50)}$) using the
202 model by Angelier (2006).

203 3. SAWC calculations

204 SAWC was determined for each of the 100 soil profiles from the collected data. We present in
205 the following the different modalities that were considered for determining each SAWC
206 components and further the combinations of modalities used to determine different possible
207 SAWC for a given soil profile.

208 3.1 Fine earth horizon AWC

209 Fine earth horizon AWC was determined for each horizon by two different methods. The first
210 was the class PTF from Al Majou (2008) that was recently recommended as the best one for
211 application in forest soil (Piedallu et al., 2018). Considering this method, $AWC_{coef(FE)}$ was
212 attributed to each horizon in function of the textural class measured in the laboratory and the
213 soil horizon type (Al Majou, 2008). The second method used a local continue PTF that was
214 computed from the 35-clods dataset. A linear regression was performed to predict the
215 measured $AWC_{coef(FE)}$ or its calculation parameters ($W_{(FC)}$, $W_{(WP)}$ and D) by using simple soil
216 properties as explanatory factors (sand, silt, clay and organic matter amount). The best model
217 among all the tested combinations predicted $AWC_{coef(FE)}$ by the following equation 4.

$$218 \text{LocalAWC}_{coef(FE)} = [(36,4934 + Sand * -0,1055) - (15,752 + OM * 0,7095)] * 0.1 \quad (4)$$

218 *Determination coefficient $R^2=0.23$; $n=35$*

219 Where $W_{(FC)}$ is the volumetric water content at field capacity, $W_{(WP)}$ is the volumetric water
220 content at wilting point, Sand is the sand content in % and OM is the organic matter content
221 in %. Considering this method, $LocalAWC_{coef(FE)}$, was calculated for each horizon.

222 3.2 Coarse fragment horizon AWC

223 Two different modalities for dealing with coarse fragment in the calculation of SAWC were
224 considered. The first was the usual one that calculates SAWC without integrating coarse
225 fraction AWC (equation 1). Such approach, comes to assume that the coarse fraction cannot

226 store available water for plant. $AWC_{coef(CF)}$ is then equal to zero, and only fine earth fraction
227 AWC is taken into account. The results of SAWC calculation that followed this modality were
228 further denoted as $SAWC_{(FE)}$. The second assumes an effective contribution of the coarse
229 fraction to the SAWC. For such method, $AWC_{coef(CF)}$ was attributed to each horizon depending
230 on the coarse fraction lithology. The results of SAWC calculation that followed this modality
231 were further denoted as $SAWC_{(total)}$.

232 3.3. Soil profile thicknesses

233 The previously mentioned equation 1 represents the contribution of soil volume in SAWC by
234 a value of thickness, which implicitly supposes that the horizons are perfectly horizontal. Thus,
235 the horizons presenting a complex geometry must be converted into an “equivalent
236 horizontal” horizon thickness, calculated as follows (equation 5).

$$237 \text{Equivalent horizon Thickness} = \frac{Vol_{(h)}}{100} \times Thickness_{(prof)} \quad (5)$$

238 Were soil thickness is expressed in mm; Vol (h) is the complex horizon volume in %;
239 $Thickness_{(prof)}$ is the thickness of the soil profile in mm.

240 SAWC was computed for different soil volumes. First, the whole soil profile volume was
241 considered. This comes to define the soil thickness (i.e. the sum of horizon thicknesses in
242 equation 1) as the distance from the soil surface to the inscrutable bedrock without
243 consideration of the rooting ($SAWC_{(Bedrock)}$). If the bedrock was too deep, the thickness limit
244 was 4.5 meters. Secondly, soil volume consisted to limit the soil thickness to an arbitrary fixed
245 value that define the maximal rooting depth beyond which the tree is not supposed to extract
246 water. Soil thicknesses of 300 cm, 200 cm, 100 cm and 50 cm were considered ($SAWC_{(300)}$,
247 $SAWC_{(200)}$, $SAWC_{(100)}$, and $SAWC_{(50)}$). By the same, a fixed floor corresponding to the depth of
the deepest observed root was also considered ($AWC_{(Max\ root\ depth)}$). Finally, an alternative

248 method for taking into account more precisely the tree root dispersion was considered.
 249 Instead of modifying the value of soil thickness, a roots density index was introduced in the
 250 AWC calculation of each horizon. This index was based on a classification derived from Baize
 251 and Jabiol (1995) presented in table 1. The mean root density used as input for this
 252 classification were calculated from the root observations performed across the 100 soil
 253 profiles.

254 *Table 1: classification of the root density at the horizon scale*

Mean root density (3 squares)	Minimum root density	Medium root density	Maximum root density	Root density index
>16 / dm ²	-	-	-	1
>8 /dm ² and <16 / dm ²	>1 0	- -	- -	1 0.75
>0 /dm ² and < 8/dm ²	0	>1 0 0	- >5 <5	0.75 0.5 0.25
0 /dm ²	0	0	0	0

255

256 3.4. The different considered SAWC

257 The different modalities for determining the three components of SAWC were combined to
 258 produce 28 estimations of SAWC, i.e. two different fine earth approaches (“Almajou2008” PTF
 259 and “local” PTF) x two different coarse fraction approaches (SAWC_(Total), SAWC_(FE)) x seven
 260 different soil volumes (Table 2).

261 *Table 2: description of the soil volumes considered for SAWC calculation*

Name	Soil volume
$AWC_{(Bedrock)}$	From soil surface to the inscrutable bedrock If Bedrock was too deep, the depth limit was 4.5 meters
$AWC_{(300)}, AWC_{(200)},$	from the surface to a fixed floor depth.
$AWC_{(100)}, AWC_{(50)}$	300 cm ; 200 cm ; 100 cm ; 50 cm
$AWC_{(Max\ root\ depth)}$	From soil surface to the deepest root observed in the pit
$AWC_{(Root\ density)}$	From soil surface to the inscrutable bedrock. AWC weighted by the horizons root density index

262

263 4. Results

264 4.1 Basic soil characteristics: average values and variability across the region

265 Table 3 presents the statistics of the main soil properties that influence SAWC. With a mean
266 of 254 mm, and exceeding 400 centimeters for some plots, the soil thickness reached
267 frequently the saprolite horizon. The studied soils showed high coarse fragments content
268 (55% at the scale of the soil profile) mainly concentrated in the saprolite horizons. The soil
269 textures were weakly variable across the study area. Most of the profiles were classified as
270 sandy loams, with high sands content resulting from the weathering of granite, gneiss,
271 sandstones and schists. Finally, soil was also characterized by an high organic matter content
272 in the surface horizons (mean = 6.0 %) that remain non negligible in S horizons (mean = 2.7%).
273 *Table 3: soil thickness, rock fragment content, clay content, silt content, sand content and*
274 *organic matter content for the different soil layers of the data set.*

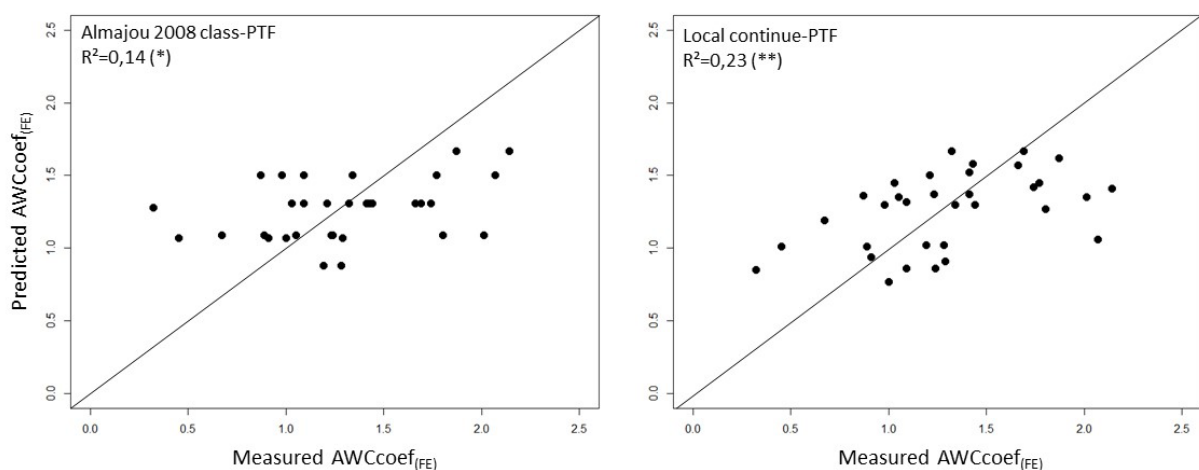
Thickness	%Coarse	Clay%	Silt%	Sand%	OM%
(mm)	fraction				

	mean	sd	mean	sd	mean	sd	mean	sd	mean	sd	mean	sd
Profile	254.0	107.0	55.5	20.0	10.3	6.8	29.3	10.6	57.3	15.7	1.1	1.0
Pedolit	67.1	29.0	21.0	16	12.9	6.6	32.1	11.1	51.0	14.7	4.7	1.9
<i>A horizon</i>	26.2	9.0	15.0	4.0	15.7	6.3	32.7	10.3	51.6	14.7	6.0	1.8
<i>S horizon</i>	36.9	21.2	27.0	22.0	11.0	7.7	33.6	13.7	55.4	18.0	2.7	1.2
Saprolit	185.4	101.0	70.9	22	9.2	7.4	27.9	11.2	60.1	17.4	0.4	0.3

275

276 4.2 Water retention of fine earth

277 Considering the 35 fine-earth clods used for the hydric property measurements, the
 278 $AWCcoef_{(FE)}$ calculated from the measured parameters ($W_{(FC)}$, $W_{(WP)}$ and D) and the
 279 $AWCcoef_{(FE)}$ estimated by Almajou PTF showed significant correlations but low coefficient of
 280 determination ($r^2=0.14$). Both $AWCcoef_{(FE)}$ varied into similar ranges, and did not showed
 281 significant differences. The $AWCcoef_{(FE)}$ estimated from the local PTF was significantly and
 282 positively correlated with the $AWCcoef_{(FE)}$ calculated from the measured hydric properties
 283 ($r^2=0.23$) (Figure 2).



284

285 *Figure 2: determination coefficients (R^2) between $AWCcoef_{(FE)}$ measured and predicted using*

286 *Almajou PTF (2008) and using the “local” PTF. N=35*

287 $AWCcoef_{(FE)}$ were estimated for each horizon of the 100 soils profiles using both local PTF and
 288 Almajou PTF. For A horizons, the $AWCcoef_{(FE)}$ estimated by the local PTF were significantly
 289 higher than the $AWCcoef_{(FE)}$ estimated by Almajou PTF. The deeper horizons showed opposite
 290 results: the $AWCcoef_{(FE)}$ estimated by local PTF showed significant lower values than those
 291 estimated with Almajou PTF.

292 4.3 Water retention of the coarse fragments

293 Results of the rock fragments hydric properties measurement showed that the samples
 294 contained available water for the trees (table 4). The $AWCcoef_{(CF)}$ varied with the lithology
 295 class of the rock fragment, with a minimum coefficient for the black schist and a maximum
 296 coefficient for the shale. Granit, gneiss and mica-schist fragments which are the main
 297 lithologic class of the studied area showed respectively $AWCcoef_{(CF)}$ of 0.58, 0.46 and 0.67.

298 *Table 4: Bulk density (D), gravimetric water content at field capacity ($W_{(FC)}$) and Wilting point*
 299 *($W_{(WP)}$), and the calculated available water capacity coefficient for coarse fraction*
 300 *($AWCcoef_{(CF)}$) for each lithologic class. N=10. sd = standard deviation*

Lithologic class	Geologic period	D	sd	$W_{(FC)}$ %	sd	$W_{(WP)}$ %	sd	$AWCcoef_{(CF)}$
Mica-schist	Cambro-Ordovician	2,09	0,13	5,55	0,76	2,33	0,47	0,67
Pelitic sandstone	Lower Cambrian	2,19	0,11	6,03	2,74	2,74	1,36	0,72
Banded sandstone	Lower Cambrian	1,87	0,04	10,9	0,46	9,3	0,28	0,30
Black schist	Lower Cambrian	2,19	0,08	4,44	0,46	3,96	0,35	0,11
Shale	Lower Cambrian	1,74	0,11	11,58	3,51	4,63	0,86	1,21
Dolomite	Lower Cambrian	2,13	0,07	3,86	1,27	2,82	0,96	0,22
Granite	Westphalian	2,27	0,09	4,26	0,59	1,7	0,54	0,58
Gneiss	Cambrian	1,93	0,2	5,78	2,01	3,39	0,78	0,46

302 4.4 Relative contribution of modalities to the variations of SAWC calculation

303 Table 5 shows the SAWC values calculated for the seven mentioned soil volumes, and
 304 following the different approaches for coarse fraction and fine earth fraction. Table 6 shows
 305 the results of the student tests assessing the effect of the coarse fraction and fine earth
 306 fraction approaches.

307 $AWC_{(Bedrock)}$ showed the highest SAWC values with a mean of 227.6mm and a maximum value
 308 reaching 547.0mm (Table 5). SAWC decreased gradually while decreasing the fixed floor
 309 depth. $AWC_{(Max\ root\ depth)}$ showed always lower values than $AWC_{(Bedrock)}$, meaning that, in
 310 average, the roots maximum depth did not reached the bedrock depth. $AWC_{(Root\ density)}$
 311 showed mean values 34 % to 45 % lower than $AWC_{(Bedrock)}$. SAWC calculated by integrating the
 312 coarse fraction AWC ($AWC_{(Total)}$) showed significant different values than AWC calculated by
 313 excluding the coarse fraction AWC ($AWC_{(FE)}$), whatever the considered soil volume (Table 6).
 314 $AWC_{(Total)}$ was always higher than $AWC_{(FE)}$ (Table 5). Considering $AWC_{(FE)}$, significant differences
 315 were only observed for the fixed floors beyond 200 cm depth. Considering the soil volume
 316 until the bedrock depth, SAWC values did not differ significantly regarding the PTF used to
 317 calculate the $AWCcoef_{(FE)}$. Result was the same considering the rooted volume, or the volume
 318 until 300- and 200-centimeters depth. However, result differed for the surface material AWC:
 319 significant differences were found between AWC values calculated from the local PTF, and
 320 AWC values calculated from the Almajou 2008 PTF (Table 6).

321 *Table 5: maximum, minimum and mean values for all the SAWC calculation. N=100*

Soil volume	$AWCcoef_{(FE)}$	$AWCcoef_{(CF)}$	Mean (mm)	Standard deviation	Minimum (mm)	Maximum (mm)
$AWC_{(Bedrock)}$	Local	$AWC_{(Total)}$	227.6	117.2	46.4	547.0

		AWC _(FE)	139.4	86.4	25.6	481.9
	Almajou	AWC _(Total)	216.0	104.3	59.5	479.2
		AWC _(FE)	131.4	69.7	29.1	376.1
AWC _(Max root depth)	Local	AWC _(Total)	192.3	93.4	35.2	489.1
		AWC _(FE)	117.6	55.2	24.9	365.2
	Almajou	AWC _(Total)	180.8	90.1	51.2	411.7
		AWC _(FE)	109.8	45.9	28.5	303.8
AWC _(Root density)	Local	AWC _(Total)	124.4	58.0	34.9	326.3
		AWC _(FE)	85.6	37.8	25.7	201.7
	Almajou	AWC _(Total)	125.9	56.1	31.5	312.0
		AWC _(FE)	86.9	38.5	21.3	208.6
AWC ₍₃₀₀₎	Local	AWC _(Total)	208.3	98.4	46.4	497.7
		AWC _(FE)	132.6	77.5	25.6	439.8
	Almajou	AWC _(Total)	198.0	87.1	59.5	465.9
		AWC _(FE)	122.3	63.1	29.1	344.7
AWC ₍₂₀₀₎	Local	AWC _(Total)	166.4	60.2	46.4	338.0
		AWC _(FE)	115.5	58.8	25.6	313.6
	Almajou	AWC _(Total)	159.4	51.7	59.5	298.0
		AWC _(FE)	108.4	48.5	29.1	250.4
AWC ₍₁₀₀₎	Local	AWC _(Total)	97.4	23.4	42.3	171.9
		AWC _(FE)	79.1	30.1	24.9	171.6
	Almajou	AWC _(Total)	96.9	18.0	41.9	141.4
		AWC _(FE)	78.5	25.2	25.5	141.1

AWC ₍₅₀₎	Local	AWC _(Total)	51.7	10.7	26.1	82.3
		AWC _(FE)	46.1	13.3	18.7	81.9
	Almajou	AWC _(Total)	55.9	8.0	26.3	71.4
		AWC _(FE)	50.3	11.4	18.9	71.1

322

323 *Table 6: effect of the PTF and coarse fraction parameters on SAWC calculation for the 7 soil*
 324 *volumes, using student test. N=100. NS= non-significant difference; significant difference at*
 325 *the 0.05 (*); 0.01 (**) and 0.001 (***) thresholds.*

326

	PTF effect	Coarse fraction effect
	Almajou Vs local PTF	AWC _(FE) Vs AWC _(Total)
AWC _(Bedrock)	NS	***
AWC _(Max root depth)	NS	***
AWC _(Root density)	NS	**
AWC ₍₃₀₀₎	NS	***
AWC ₍₂₀₀₎	NS	***
AWC ₍₁₀₀₎	*	***
AWC ₍₅₀₎	**	**

327

328 4.5 Relation with tree growth

329 Site fertility index, measured by H₅₀ showed a mean of 35.4 meters high and a standard
 330 deviation of 3.6. The most fertile plot reached a H₅₀ of 44.6 m while the lowest fertility index
 331 was 26.8 m.

332 Table 7: Spearman's correlation coefficients between the fertility index (H_{50}) and SAWC
 333 calculated for the 7 soil volumes, including $AWC_{(CF)}$ ($AWC_{(Total)}$) or excluding it ($AWC_{(FE)}$), and
 334 using the local PTF or Almajou PTF for $AWC_{coef_{(FE)}}$ estimation. $N=100$. NS= non-significant
 335 difference ; significant difference at the 0.05 (*) ; 0.01 (**) and 0.001 (***) thresholds.

SAWC	$AWC_{coef_{(CF)}}$	$AWC_{coef_{(FE)}}$			
		Almajou PTF		Local PTF	
$AWC_{(Bedrock)}$	$AWC_{(Total)}$	0.47	***	0.48	***
	$AWC_{(FE)}$	0.40	***	0.42	***
$AWC_{(Max\ root\ depth)}$	$AWC_{(Total)}$	0.32	**	0.35	**
	$AWC_{(FE)}$	0.30	**	0.31	**
$AWC_{(Root\ density)}$	$AWC_{(Total)}$	0.29	**	0.31	**
	$AWC_{(FE)}$	0.25	*	0.26	*
$AWC_{(300)}$	$AWC_{(Total)}$	0.44	***	0.48	***
	$AWC_{(FE)}$	0.37	**	0.40	***
$AWC_{(200)}$	$AWC_{(Total)}$	0.42	***	0.45	***
	$AWC_{(FE)}$	0.34	**	0.37	**
$AWC_{(100)}$	$AWC_{(Total)}$	0.35	**	0.37	**
	$AWC_{(FE)}$	0.28	*	0.29	*
$AWC_{(50)}$	$AWC_{(Total)}$	0.26	*	0.28	*
	$AWC_{(FE)}$	0.18	NS	0.24	*

336
 337 SAWC correlated significantly and positively with H_{50} whatever the considered soil volume
 338 except for $AWC_{(50)}$. The best correlation coefficients were found for the greatest volumes of
 339 soil without including the rooting effect ($AWC_{(Bedrock)}$, $AWC_{(300)}$ and $AWC_{(200)}$). Whatever the

340 considered material, SAWC showed better correlation coefficient with H_{50} when it included
341 the $AWC_{(CF)}$. The effect of the chosen PTF for estimating the $AWC_{(FE)}$ did not alter the
342 relationship between SAWC and H_{50} : correlation coefficients were not significantly different.

343 **5. Discussion**

344 5.1 Fine earth water retention

345 The forest soils considered for the present study showed relative homogeneous sandy texture,
346 high organic matter content. Such soil properties induced specific water retention behavior
347 for the fine earth that were found to be very hardly predicted by using Almajou PTF. Indeed,
348 while the Almajou PTF predicted homogeneous $AWC_{coef_{(FE)}}$, the coefficients based on the
349 measured values showed higher variability, especially for the surface horizons.

350 Texture, as an only factor, might not be able to predict water retention for the studied soils.
351 It seems that organic matter content may play an important role. Indeed, such relationship
352 was partly found by using the continue local PTF. However, even if the relationship was
353 statistically significant, it only allowed to predict 23 % of the measured water retention
354 variability. This lack of performance can be explained by the low number of samples used in
355 this study (35) combined with a low range of water retention properties ($W_{(FC)}$, $W_{(WP)}$) in
356 comparison to other studies (ref).

357 Anyway, the fine earth retention seems not to impact less the variation of SAWC than other
358 factors. As an explanation, the volume of fine earth has a very homogeneous soil texture.
359 Furthermore, it is smaller than usually measured due to the richness in coarse fragments, and
360 the increase of coarse fragment with depth result in a decrease of fine earth AWC impact. As
361 a conclusion, the increase of variations of other AWC components than fine earth may explain
362 this weak importance. However, it should be tried in more texture contrasted pedological
363 context. It is also worth noting that recommended PTF failed to represent the fine earth

364 retention variability and that the local PTF stress the negative impact of organic matter on the
365 wilting point, which, to our knowledge have never been encountered in studies dealing with
366 agricultural soils. This re-enforce the need of specific PTF for forest soils.

367 5.2 Retention of coarse fragment

368 The water retention capacity of coarse fragment based on measurements was found
369 important to take into account for explaining tree growth. The correlation coefficients raised
370 significantly whatever the considered soil volume with however greater differences when
371 deeper layers were considered. It is explained by the importance of coarse fragment,
372 especially in the saprolite zone, but also to the substantial water retention of some of the
373 pebbles.

374 Indeed, we measured $AWC_{coef(CF)}$ varying between 0.11 and 1.21 depending on the rock
375 fragment lithology. This is consistent with previous studies (Tetegan et al., 2011; Parajuli et
376 al., 2017). Parajuli et al., 2017 showed that the water retention capacity of sandstones
377 fragment was linked to the sample porosity. Tetegan et al. studied the water retention
378 capacities of different types of sedimentary rocks. They found that the $AWC_{(CF)}$ depends on
379 the rock fragment bulk density, with the higher $AWC_{coef(CF)}$ for bulk density varying between
380 1.5 and 1.8. The results of the present study for $AWC_{coef(CF)}$ values were very similar, even if
381 the lithologic nature of the studied samples was very different. Considering the studied soils,
382 the $AWC_{(CF)}$ represented 39 % of the $AWC_{(Total)}$ for the $AWC_{(Bedrock)}$ and 31 % for the $AWC_{(200)}$.
383 We recommend that water retention of coarse fragment could be also accounted for. The
384 variability shown in this study suggest that PTF should also be built for coarse fraction, and
385 especially for the weathered rock fragment showing a low bulk density and high porosity.
386 Finally, this result also underlined the crucial importance of a precise assessment of the coarse

387 fraction volume within the soil profile. A 2cm- sieving and weighing performed in the field
388 appeared to be a progress from classical visual estimations from the profile wall.

389 5.3 Soil Volume

390 Soil volume seems to be the main driver of SAWC in our study area. We showed that for
391 Douglas-fir fertility index, the best correlation coefficients were obtained with SAWC
392 calculated on the thickest and deepest materials: $AWC_{(Bedrock)}$, $AWC_{(300)}$ and $AWC_{(200)}$. Anyway,
393 with correlation coefficients quite similar than $AWC_{(Bedrock)}$, $AWC_{(200)}$ seemed to be deep and
394 thick enough for accounting for the soil impact on the tree growth. This might mean that the
395 critical AWC layer for tree fertility was not the global and potentially rooted saprolite zone,
396 but a thinner volume of material that concentrated the higher root density (Brantley et al.,
397 2017). In this way, the SAWCs taking into account direct observations of rooting depths ($AWC_{(Max\ root\ depth)}$, $AWC_{(Root\ density)}$) would have been theoretically the best methods for assessing
398 SAWC. Indeed, root distribution is like a map of where water is most likely to be present during
399 the growing season (Brantley et al., 2017). Curt et al., 1998 proposed a typology for the root-
400 system architecture of Douglas-fir that was strongly correlated with Douglas-fir fertility index
401 (H_{25}). However, it was not the case for the present study. The correlation coefficients with H_{50}
402 were lower for the SAWC weighted on the root density than for SAWC based on fixed floor
403 depth. This can be explained by the difficulty in observing functional roots that are very thin
404 (diameter <1mm) and by the omission of mycorrhizal effect.

406 Finally, the lower correlation coefficients were found for the surface material $AWC_{(100)}$ and
407 $AWC_{(50)}$. Such material seemed to be not thick and deep enough to precisely characterize the
408 SAWC potential for a given site. This result questions the common field method for SAWC
409 assessment that used manual auger to probe the soil with a very limited depth.

410 5.4 AWC – tree growth relation

411 The SAWC-tree growth relation was found significant with SAWC explaining at best 23% of
412 the H_{50} variability. Many studies explored the relationships between tree growth and SAWC.
413 Piedallu et al. (2011) showed that SAWC calculated by using manual auger, Almajou PTF for
414 estimating $AWC_{(FE)}$, and without including the coarse fraction AWC could explained at most 12
415 % of the fertility index of *Fagus sylvatica*, *Picea Abies* and *Quercus Petraea*. Curt et al., (2001)
416 showed that SAWC explained 29 % of Douglas-fir growth in the Limousin (French Massif
417 Central). For this study, SAWC was calculated on 1-meter depth pit using by the “texture
418 method” (Baize & Jabiol, 1995), and Douglas-fir growth was estimated at the reference age of
419 25 years. This stronger relationship for Curt et al. (2001) can be explained by a more
420 homogeneous climate and geology of the studied area than ours. Indeed, for the Haut-
421 Languedoc area, the climatic confluence situation and the geological heterogeneity induced
422 very complex interactions between the Douglas-fir growth factors. Climate variables such as
423 an early vegetative season water deficit (Sergent et al., 2012) and other factors such as
424 chemical fertility, former land use (Curt et al., 2001), or genetic origin of Douglas-fir trees
425 (Bansal et al., 2015) may also play an important role. SAWC appeared as a complementary
426 factor, but can be more useful when the first-order factors such as climate remain weakly
427 variable.

428 **6. Conclusion**

429 SAWC concept which was created for agricultural soils requires specific adaptations when it is
430 estimated for forest soils. The present study pointed three possible improvements for forest
431 SAWC assessment: 1) the development of specific PTF for forest soils, integrating texture and
432 organic matter content as explanatory factors for fine earth water retention properties, 2) the
433 integration of the coarse fraction AWC for SAWC calculation and thus, the development of
434 rock fragment PTF, and 3) the consideration of a 200cm deep soil volume for SAWC

435 assessment. This last point appears to be the most difficult to practically take into account in
436 usual field sampling devices, because the digging of such a soil volume is expansive. Thus, the
437 modelling of the total soil thickness by using available surface and subsurface indicators could
438 be a crucial issue for forest soil AWC assessment.

439 **Acknowledgement**

440 We are grateful to the LIFE FORECCAsT project (LIFE15 CCA/FR/000021) who supported and
441 managed this work. We gratefully thank Jérôme Gouin (GeSolEau) for the soil profile description
442 and sampling, Evrard Gutkin for the soil pit digging and filling. This study would not be possible
443 without the help of the agents of the CRPF Occitanie and without the agreement of the forest
444 owners.

445 **References**

- 446 Al Majou, H., Bruand, A., Duval, O., 2008. The use of in situ volumetric water content at field
447 capacity to improve the prediction of soil water retention properties. *Canadian Journal of Soil*
448 *Science* 88, 533–541.
- 449 Angelier, A., 2006. Guide des sylvicultures pour le Douglas : de nouvelles courbes de fertilité
450 adaptées. *Rendez-vous techniques*. Office national des forêts 11, 7-12.
- 451 Baize, D., Jabiol, B., 1995. Guide pour la description des sols. INRA, Paris.
- 452 Bansal, Harrington, C., Gould, P., St Clair, J.B., 2015. Climate-related genetic variation in drought-
453 resistance of Douglas-fir (*Pseudotsuga menziesii*). *Global Change Biology*, 21(2),947-58. doi:
454 10.1111/gcb.12719.
- 455 Breda, N., Huc, R., Granier, A., Dreyer, E., 2006. Temperate forest trees and stands under severe
456 drought: a review of ecophysiological responses, adaptation processes and long-term
457 consequences. *Annals of Forest Science* 63, 625–644.

458 Bruand, A., Fernandez, P.N., Duval, O., 2003. Use of class pedotransfer functions based on texture
459 and bulk density of clods to generate water retention curves. *Soil Use and Management* 19, 232–
460 242.

461 Chen, H.Y.H., Krestov, P.V., Klinka, K., 2002. Trembling aspen site index in relation to
462 environmental measures of site quality at two spatial scales. *Canadian Journal of Forest Research*
463 -*Revue Canadienne De Recherche Forestiere* 32, 112–119.

464 Cousin, I., Nicoullaud, B., Coutadeur, C., 2003. Influence of rock fragments on the water retention
465 and water percolation in a calcareous soil. *Catena* 53, 97–114.

466 Curt, T., Bouchaud, M., Agrech, G., 2001. Predicting site index of Douglas-Fir plantations from
467 ecological variables in the Massif Central area of France. *Forest Ecology and Management* 149,
468 61–74.

469 Curt, T., Bouchaud, M., Lucot, E., Bardonnet, C., Bouquet, F., 1998. Influence des conditions
470 géopédologiques sur le système racinaire et la croissance en hauteur du Douglas dans les monts
471 du Beaujolais. *Ingénieries - E A T, IRSTEA*, 29 - 46.

472 Dominati, E., Mackay, A., Green, S., Patterson, M., 2014. A soil change-based methodology for the
473 quantification and valuation of ecosystem services from agro-ecosystems: a case study of pastoral
474 agriculture in New Zealand. *Ecological Economics. Econ.* 100, 119–129.

475 Graham, R. C., Rossi, A. M., Hubbert, K. R., 2010. Rock to regolith conversion: producing hospitable
476 substrates for terrestrial ecosystems, *GSA Today* 20, 4–9.

477 Granier, A., Bréda, N., Biron, P., Villette, S., 1999. A lumped water balance model to evaluate
478 duration and intensity of drought constraints in forest stands. *Ecological Modelling*, 116, 269–283.

479 Infosol, 2018. Donesol version 3.7. Dictionnaire de données. GISSOL, Orléans, 492 pp

480 Jamagne, M., Betremieux, R., Begon, J.C., Mori, A., 1977. Quelques données sur la variabilité dans
481 le milieu naturel de la réserve en eau des sols. *agro - INRA* 127, 627–641.

482 Lebourgeois, F., Bréda, N., Ulrich, E., Granier, A., 2005. Climate-tree-growth relationships of
483 European beech (*Fagus sylvatica* L.) in the French Permanent Plot Network (RENECOFOR). *Trees*
484 *Structure and Function* 19, 385–401.

485 Littke K., Zabowski D., Turnblom E., Harrison R., 2018. Estimating shallow soil available water
486 supply for Douglas-fir forests of the coastal Pacific Northwest: climate change impacts. *Canadian*
487 *Journal of Forest Research*, 48(4), 421-430. <https://doi.org/10.1139/cjfr-2017-0385>

488 Parajuli K., Sadeghi M., Jones S.B., 2017. A binary mixing model for characterizing stony-soil water
489 retention. *Agricultural and Forest Meteorology* 1–8, 244–245.

490 Piedallu C., Gégout J.-C., Bruand A., Seynave I., 2011. Mapping soil water holding capacity over
491 large areas to predict potential production of forest stands. *Geoderma*, 160(3): 355-366.

492 Piedallu, C., Pousse, N., Bruand, A., Dietz, L., Figuepron, J., 2018. Estimer le réservoir en eau des
493 sols. Quelles fonctions de pédotransfert le forestier doit-il utiliser ? *Forêt-entreprise* , 242, 28-32.

494 Sergent, A. S., Rozenberg, P., Bréda, N., 2012. Douglas-fir is vulnerable to exceptional and
495 recurrent drought episodes and recovers less well on less fertile sites. *Annals of Forest Science* 71,
496 697–708. DOI 10.1007/s13595-012-0220-5.

497 Seynave, I., Gégout, J.-C., Hervé, J.-C., Dhôte, J.-F., Drapier, J., Bruno, É., Dumé, G., 2005. *Picea*
498 *abies* site index prediction by environmental factors and understorey vegetation: a two-scale
499 approach based on survey databases. *Canadian Journal of Forest Research*, 35(7), 1669–1678.
500 doi:10.1139/x05-088

501 Steiger, J.H., 1980. Tests for comparing elements of a correlation matrix, *Psychological*
502 *Bulletin*, 87, 245-251.

503 Veihmayer, F.J., Hendrickson, A.H., 1927. Soil moisture conditions in relation to plant growth.
504 *Plant Physiology*, Lancaster, 2, 71–82.

505 Vincke, C., Delvaux, B., 2005. Porosity and available water of temporarily waterlogged soils in
506 a *Quercus robur* (L.) declining stand. *Plant and Soil* 271, 189–203.

507 Wösten, J.H.M., Pachepsky, Y.A., Rawls, W.J., 2001. Pedotransfer functions: bridging the gap
508 between available basic soil data and missing soil hydraulic characteristics. *Journal of*
509 *Hydrology (Amsterdam)* 251, 123–150.